J Comp Physiol B
DOI 10.1007/s00360-017-1106-5

ORIGINAL PAPER

Comparative physiology of vocal musculature in two odontocetes, the bottlenose dolphin (*Tursiops truncatus*) and the harbor porpoise (*Phocoena phocoena*)

Nicole M. Thometz[1,2] · Jennifer L. Dearolf[3] · Robin C. Dunkin[2] · Dawn P. Noren[4] · Marla M. Holt[4] · Olivia C. Sims[3] · Brandon C. Cathey[3] · Terrie M. Williams[2]

Received: 31 January 2017 / Accepted: 11 May 2017

Abstract The mechanism by which odontocetes produce sound is unique among mammals. To gain insight into the physiological properties that support sound production in toothed whales, we examined myoglobin content ([Mb]), non-bicarbonate buffering capacity (β), fiber-type profiles, and myosin heavy chain expression of vocal musculature in two odontocetes: the bottlenose dolphin (*Tursiops truncatus;* $n = 4$) and the harbor porpoise (*Phocoena phocoena;* $n = 5$). Both species use the same anatomical structures to produce sound, but differ markedly in their vocal repertoires. *Tursiops* produce both broadband clicks and tonal whistles, while *Phocoena* only produce higher frequency clicks. Specific muscles examined in this study included: (1) the nasal musculature around the phonic lips on the right (RNM) and left (LNM) sides of the head, (2) the palatopharyngeal sphincter (PPS), which surrounds the larynx and aids in pressurizing cranial air spaces, and (3) the genioglossus complex (GGC), a group of muscles positioned ventrally within the head. Overall, vocal muscles had significantly lower [Mb] and β than locomotor muscles from the same species. The PPS was predominately composed of small diameter slow-twitch fibers. Fiber-type and myosin heavy chain analyses revealed that the GGC was comprised largely of fast-twitch fibers (*Tursiops*: 88.6%, *Phocoena*: 79.7%) and had the highest β of all vocal muscles. Notably, there was a significant difference in [Mb] between the RNM and LNM in *Tursiops*, but not *Phocoena*. Our results reveal shared physiological characteristics of individual vocal muscles across species that enhance our understanding of key functional roles, as well as species-specific differences which appear to reflect differences in vocal capacities.

Keywords Aerobic metabolism · Anaerobic capacity · Myoglobin · Fiber-type · Myosin heavy chain · Sound production

Communicated by G. Heldmaier.

✉ Nicole M. Thometz
nthometz@usfca.edu

[1] Department of Biology, University of San Francisco, 2130 Fulton St, San Francisco, CA 94117, USA

[2] Department of Ecology and Evolutionary Biology, Long Marine Laboratory, University of California at Santa Cruz, 115 McAllister Way, Santa Cruz, CA 95060, USA

[3] Biology Department, Hendrix College, 1600 Washington Ave., Conway, AR 72032, USA

[4] Conservation Biology Division, Northwest Fisheries Science Center, National Marine Fisheries Service, National Oceanic and Atmospheric Administration, 2725 Montlake Boulevard East, Seattle, WA 98112, USA

Introduction

The majority of mammalian species produce sound via the larynx. In general, the coupled movement of a muscular diaphragm and air-filled lungs provides the means to pressurize air within the respiratory system. The movement of air past vocal cords located within the larynx and the resulting vibration of the vocal cords is the mechanism by which sound is produced (Bradbury and Vehrencamp 1998). Odontocetes, also known as toothed whales, are a unique exception to this typical model of mammalian sound production.

This group of exclusively aquatic mammals, which includes dolphins and porpoises, have evolved to produce sound using a complex nasal system, rather than the larynx (Tyack and Miller 2002). This system, located above the

Published online: 31 May 2017

rostrum in toothed whales, consists of pressurized air sacs, connective tissue, specialized lipids, and skeletal muscle (Mead 1975; Houser et al. 2004). Contraction of skeletal muscles within the head pressurizes the nasal cavities (Dormer 1979; Green et al. 1980; Amundin and Andersen 1983), an action required to effectively move air from the bony nares, past paired structures known as phonic lips, and into vestibular air sacs (Cranford et al. 1996; Huggenberger et al. 2009). Vibration of the phonic lips, caused by air flow through the nasal system, is the mechanism by which odontocetes produce sound (Dormer 1979; Cranford et al. 1996, 2011). On a breath hold, subsequently, air can be recycled within the nasal system via the relaxation of vocal muscles and associated structures (Dormer 1979; Amundin and Andersen 1983). Although all toothed whales produce sound using this same basic mechanism, the type and complexity of sounds produced vary distinctly by species (Mead 1975; Cranford et al. 1996; Au et al. 2006; Madsen et al. 2010; Ridgway et al. 2015).

Odontocetes produce sound for a variety of reasons, including echolocation (i.e., searching for and locating prey) and communication (e.g., socializing and finding mates); and are capable of producing a wide array of complex sounds (Tyack and Miller 2002; Au et al. 2006; Lammers and Castellote 2009; Madsen et al. 2010, 2013). They produce these sounds on a breath hold while underwater, where they necessarily must exercise (e.g., traveling, diving, and foraging) and vocalize simultaneously. Consequently, exercise and sound production must be fueled by the same exhaustible onboard oxygen stores (Ponganis 2011), making the ability to store and efficiently use oxygen while breath-holding of critical importance to locomotion, foraging, and communication. In addition, a suite of specialized ventilatory muscles must work in concert to facilitate rapid gas exchange at the surface (Cotten et al. 2008). Locomotor costs are often the only consideration when modeling oxygen depletion during diving in marine mammals (Kooyman 1989; Castellini et al. 1992; Burns and Castellini 1996; Noren et al. 2002; Richmond et al. 2006; Yeates et al. 2007; Williams et al. 2011a; Shero et al. 2012), despite the fact that rapid ventilation and sound production are also energetic processes which rely on specialized skeletal muscles (Cotten et al. 2008; Gillooly and Ophir 2010; Ophir et al. 2010; Piscitelli et al. 2010).

The metabolic cost of sound production in cetaceans has been found to vary by the type of sound and the sound energy level (Noren et al. 2013; Holt et al. 2015). As anthropogenic noise in the oceans continues to increase (Hildebrand 2009), the vocal behavior of many marine species will likely change in response (Weilgart 2007; Melcón et al. 2012), which may increase the daily energy expenditure of individuals that must vocalize more often and/or louder to compensate. Although sound production is hypothesized to be a relatively low-cost activity for odontocetes (Dunkin et al. in prep), the energetic cost of sound production has only been empirically examined in a single species under a subset of controlled conditions (Noren et al. 2013; Holt et al. 2015). Thus, examining the metabolic pathways and physiological characteristics that support sound production in toothed whales can provide novel insight into the potential impacts of increasing oceanic noise and resulting modifications in individual behavior.

A number of studies have conducted in-depth physiological and biochemical examinations of cetacean locomotor muscles (Blessing 1972; Ponganis and Pierce 1978; Dolar et al. 1999; Noren and Williams 2000; Dearolf et al. 2000; Noren 2004; Williams et al. 2011b; Velten et al. 2013; Kielhorn et al. 2013; Noren et al. 2014; Cartwright et al. 2016). These studies have illustrated how structural and biochemical characteristics of locomotor muscles help to define species-specific diving and foraging capacities. However, within species, the physiological properties of different skeletal muscle groups are not homogenous. Indeed, in a number of terrestrial and marine species, differences in myoglobin content, enzyme activity, mitochondrial density, fiber-type profiles, and other physiological properties have been documented between major locomotor muscles (e.g., quadriceps, longissimus dorsi, and pectoralis) and other skeletal muscles (e.g., rectus abdominus, diaphragm, and sternohyoid) (Pattengale and Holloszy 1967; Blessing 1972; Ponganis and Pierce 1978; Turner and Butler 1988; Ponganis et al. 1997; Dolar et al. 1999; Kanatous et al. 1999; Dearolf 2003; Cotten et al. 2008).

In this study, we examine a suite of biochemical and morphological properties of a number of skeletal muscles believed to play key roles in pressurization of and/or air movement within the nasal complex, and thus sound production, in two species of toothed whales: the bottlenose dolphin (*Tursiops truncatus*) and the harbor porpoise (*Phocoena phocoena*). Specifically, we examine the nasal musculature surrounding the phonic lips on both the right (RNM) and left (LNM) sides of the head. The RNM and LNM consist of five highly interconnected, fan-shaped muscles that work together to modify the conformation of air spaces and facilitate air movement within the nasal complex during sound production (Mead 1975). In addition, we examine the palatopharyngeal sphincter (PPS) and the genioglossus complex (GGC). The PPS is a sphincter muscle that surrounds the larynx and aids in pressurizing cranial air spaces; a critical component of odontocete sound production (Lawrence and Schevill 1965; Green et al. 1980; Houser et al. 2004; Huggenberger et al. 2008). In contrast, the GGC is located ventrally within the head and is comprised of three distinct muscles, all of which are believed to be involved in sound production (via control of air movement within the nasal

complex) and prey consumption (Lawrence and Schevill 1956; Liste et al. 2006; Werth 2007; Huggenberger et al. 2009). Combined, the unique movements of these muscles facilitate sound production in toothed whales.

The goal of this research is to describe the physiological properties of odontocete vocal muscles to gain a better understanding of their structure and function. Although the two target species use the same anatomical machinery to produce sound (Lawrence and Schevill 1956; Mead 1975), they differ greatly in their vocal repertoires. *Tursiops* are capable of highly complex vocalizations, producing both broadband clicks and tonal whistles, and are able to produce both sound types simultaneously (Madsen et al. 2013; Ridgway et al. 2015). In contrast, *Phocoena* only produce narrower band, higher frequency clicks (Au et al. 2006; Madsen et al. 2010). Furthermore, asymmetrical cranial morphology has been documented in *Tursiops* (Mead 1975; Dormer 1979), but not *Phocoena*; and it has been well established that *Tursiops* produce clicks from the right side of the head and whistles from the left (Mead 1975; Dormer 1979; Madsen et al. 2013).

We hypothesize that the biochemical and morphological characteristics of vocal muscles will differ within and across species. We predict that differences among vocal muscle groups will reflect their distinct roles in sound production. Overall, we anticipate that the physiological properties of vocal and locomotor skeletal muscles will differ based on the relatively low cost of sound production (Noren et al. 2013; Holt et al. 2015) in comparison to locomotor costs (Williams et al. 1993; Williams 1999) in toothed whales. Finally, given the documented differences in cranial anatomy and vocal repertoires, we predict differences in the muscle physiology between the RNM and LNM in *Tursiops*, but not *Phocoena*.

Materials and methods

Specimens

Whole or partial (e.g. head only) carcasses of Atlantic bottlenose dolphins (*Tursiops truncatus; n* = 4) and Pacific harbor porpoises (*Phocoena phocoena; n* = 5) were obtained through marine mammal stranding networks on both the east and west coasts of the United States, respectively (Table 1). Only samples from sexually mature (adult or sub-adult) animals, in code 2 (fresh) condition, with the head reasonably intact (i.e. minimal external trauma, decomposition, or scavenging), and skeletal muscles free of excessive hemorrhaging were included in this study.

Muscle selection, sampling, and storage

Detailed dissections (Fig. 1) were conducted on all study animals to identify and retrieve target muscles. Muscles of interest were those known, or thought to play a role in sound production and could reliably be identified and sampled in individuals of both species. Due to the complex and interconnected nature of the skeletal musculature of cetacean heads (Lawrence and Schevill 1965; Mead 1975; Green et al. 1980), when appropriate, vocal muscle groups rather than individual muscles were selected for sampling and analysis.

The target muscle groups determined for the dorsal side of the head were the right and left nasal musculature (RNM and LNM) surrounding the phonic lips (Fig. 1a, b), which included the posterior externus, anterior externus, posterior internus, anterior internus, and intermedius muscles on either side of the head (Mead 1975). Target muscles on the ventral side of the head (Fig. 1c, d) were the palatopharyngeal sphincter (PPS) and genioglossus complex (GGC). The PPS surrounds

Table 1 Description of cetacean specimens used in this study

Specimen ID	Carcass origin	Species	Sex	Age class	Straight length (cm)	Muscles collected
WAM628	Oak Island, NC	*T. truncatus*	F	Adult	246	RNM, LNM, PPS, GGC
SWT001	Holden Beach, NC	*T. truncatus*	M	Sub-adult	244	RNM, LNM, PPS
KLC156	Carova, NC	*T. truncatus*	M	Sub-adult	225.5	RNM, LNM, PPS, GGC
WAM650	Oak Island, NC	*T. truncatus*	M	Sub-adult	210	RNM, LNM, PPS, GGC
LMLPp2014	Watsonville, CA	*P. phocoena*	F	Adult	171	PPS
C464	San Luis Obispo, CA	*P. phocoena*	F	Adult	166	RNM, LNM
CRC1475	Ocean City, WA	*P. phocoena*	F	Adult	165	RNM, LNM, PPS, GGC, LD
SJC0025	San Diego, CA	*P. phocoena*	M	Adult	158	RNM, LNM, PPS, GGC, LD
C458	San Francisco, CA	*P. phocoena*	F	Sub-adult	120	RNM, LNM, PPS, GGC

Muscles collected include: *RNM* right nasal musculature, *LNM* left nasal musculature, *PPS* palatopharyngeal sphincter, *GGC* genioglossus complex, *LD* longissimus dorsi

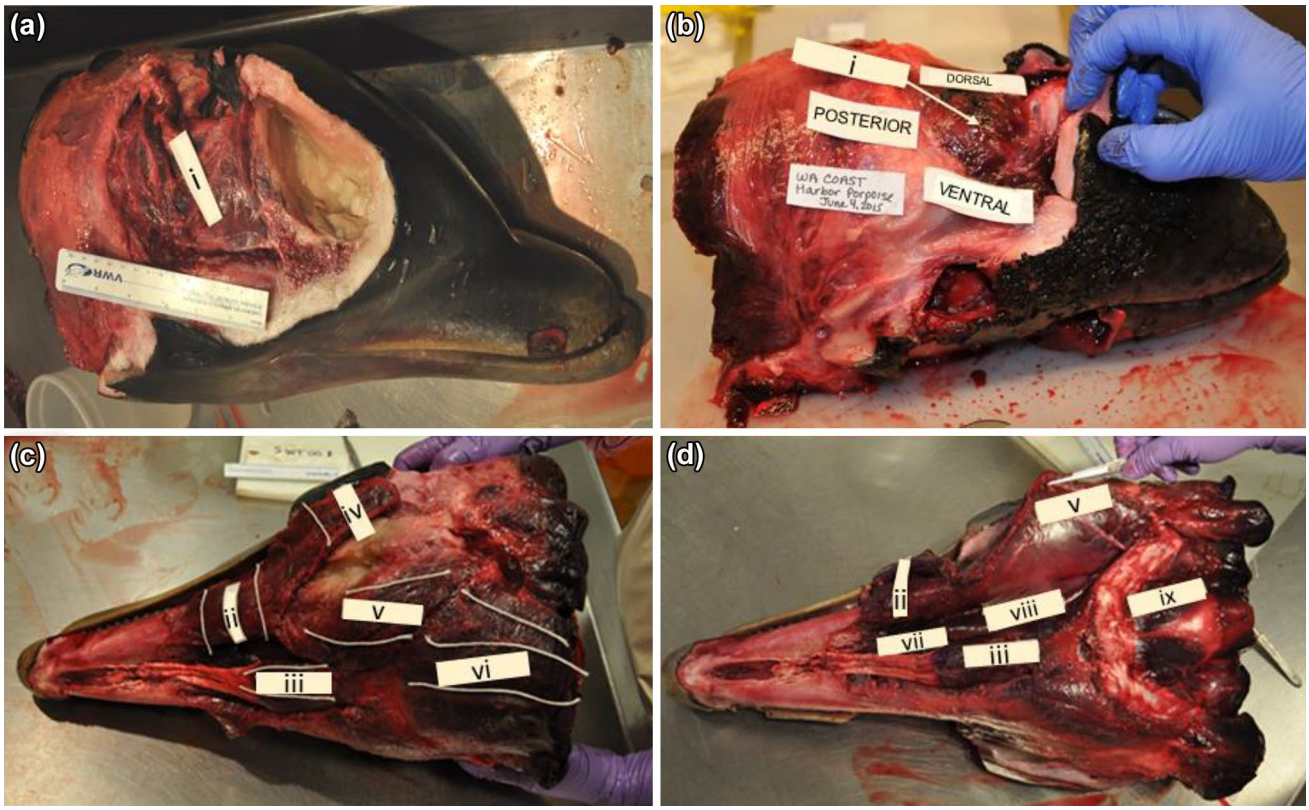

Fig. 1 Representative images of detailed cetacean head dissections when sampling target sound production muscles. **a** Dorsal view of right side of *Tursiops truncatus* head. **b** Dorsal view of right side of *Phocena phocoena* head. **c** Ventral side of *Tursiops truncatus* head showing superficial muscle groups. **d** Ventral side of *Tursiops truncatus* head identifying deeper muscle groups. Roman numerals denote specific muscles and muscle groups: (*i*) right nasal musculature, (*ii*) mylohyoid, (*iii*) geniohyoid, (*iv*) platysma, (*v*) digastric, (*vi*) sternohyoid, (*vii*) genioglossus, (*viii*) hyoglossus and styloglossus, and (*ix*) thyrohyoid

the larynx and is involved in pressurizing air within the nasal complex during sound production (Lawrence and Schevill 1965; Green et al. 1980; Houser et al. 2004). The GGC, comprised of the genioglossus, hyoglossus, and styloglossus muscles, is believed to be involved in both sound production, via controlling movement of air within the nasal complex, and prey consumption (Lawrence and Schevill 1956; Liste et al. 2006; Werth 2007; Huggenberger et al. 2008, 2009). When available, matched locomotor muscle (longissimus dorsi) samples were collected to be used for comparison.

Not all target muscles or muscle groups could be obtained from each individual due to a variety of factors (e.g., isolated physical damage, bruising, or decomposition, only head available for dissection, etc.). Specific muscle samples obtained from each individual are identified in Table 1. All muscle samples were either wrapped in foil and placed in Ziploc® freezer bags or placed in Whirl-Pacs®, and stored at −80 °C until analyses were conducted.

Biochemical analyses

To examine the relative aerobic and anaerobic capacities of vocal musculature in each species, we determined the myoglobin content ([Mb]) and acid buffering capacity (β) due to non-bicarbonate buffers of collected samples following the methods of Reynafarje (1963) and Castellini and Somero (1981), respectively. For myoglobin analyses, samples were thawed, blotted dry, and cleared of any connective tissue. Approximately 0.25–0.35 g of muscle was cut, weighed (XS2002S scale, Mettler-Toledo), and minced with a straight-edge razor before being placed in a centrifuge tube on ice. Next, a low ionic strength buffer (0.04 M phosphate) was added to each tube using a buffer-to-tissue ratio of 39.25 mL buffer per gram of wet tissue. Once buffer was added, samples were minced again using surgical scissors and sonicated (Sonifier Cell Disruptor Model 450, Branson Ultrasonics, Danbury, CT, USA) for 3 min while on ice. A blank containing only buffer solution was prepared alongside all samples.

All tubes were spun at 28,000 G for 50 min at 0–2 °C in an ultracentrifuge (Sorvell RC-5B Refrigerated Superspeed Centrifuge, DuPont Instruments). Supernatant (3 mL) was transferred into test tubes and bubbled with carbon monoxide (CO) for 8 min. Sodium dithionite (0.02–0.03 g) was added to each test tube and samples were bubbled with CO for another 2 min to ensure complete reduction. The absorbance of each sample at 538 and 568 nm was read using a spectrophotometer (BioSpec-1601, UV–visible spectrophotometer, Shimadzu Corporation, Kyoto, Japan). All samples were run in triplicate and [Mb] reported in units of g Mb per 100 g wet tissue. Sea otter (*Enhydra lutris*) locomotor muscle of known [Mb] was used as an assay control. All values are reported as means ± standard errors.

To determine the acid buffering capacity of muscle due to non-bicarbonate buffers, frozen samples were thawed, blotted dry, and cleared of any connective tissue as described for Mb analyses. Approximately 0.5 g of muscle was cut, weighed (XS2002S scale, Mettler-Toledo), minced, and placed in 40 mL scintillation vials on ice. Next, 10 mL of normal saline solution (0.9% NaCl) was added to each vial, and samples were minced with surgical scissors and sonicated (Sonifier Cell Disruptor Model 450, Branson Ultrasonics, Danbury, CT, USA) on ice for 3 min. All vials were placed in a 37 °C water bath following sonication and allowed to equilibrate.

Samples were maintained at 37 °C while titrated with 0.2 N NaOH using a repeater pipette at a rate of 20 µL of NaOH. A benchtop pH meter (pH/mV/°C 510 Series Benchtop Meter, Oakton Instruments, Vernon Hills, IL, USA) equipped with a pH electrode and ATC probe (Oakton Instruments, Vernon Hills, IL, USA) was used to monitor changes in pH throughout titration. Buffering capacity due to non-bicarbonate buffers was measured in slykes (β), which is defined as the µmoles of base necessary to increase the pH of a sample by 1 pH unit per gram wet muscle, over the pH range of 6.0–7.0. All samples were run in triplicate. β values are reported as means ± standard errors.

Muscle histochemistry

Four samples (approximately 1 cm^3) of each muscle (Table 1) were mounted on cork blocks wrapped in aluminum foil with Tissue Freezing Medium (Thermo Fischer Scientific, Waltham, MA, USA), and snap frozen in isopentane cooled to −150 °C in liquid nitrogen. *Tursiops* muscle samples were frozen for 5, 10, 15, and 20 s (one sample/freezing time), and *Phocoena* muscle samples were frozen for 6, 9, 12, and 15 s. Subsequently, individual samples were immediately placed in 15 mL Nalgene cryogenic vials that had been sitting on dry ice for >30 min before sample preparation. Once the isopentane evaporated, each vial was capped and stored in a −70 °C freezer until analysis.

In preparation for cutting, samples were placed in a −20 °C cryostat (Leica 1850, Leica Biosystems, Buffalo, IL, USA) for at least 1 h. Samples were then mounted on chucks with Tissue Freezing Medium and quick frozen with Fisherbrand Super Friendly Freeze'It® Spray. Seven and nine micrometer-thick sections of each muscle were cut and placed on Fisherbrand Superfrost Plus® slides. Muscle sections were stained for myosin ATPase activity under acidic and alkaline conditions (Hermanson and Hurley 1990). One set of sections was pre-incubated in a series of acidic solutions [pH 4.1–4.7 (0.1 increments); 40 mM barbital acetate buffer, 43 mM HCl] for 5 min at 37 °C and then rinsed for 3 min in sodium barbital buffer (20 mM sodium barbital, 13 mM $CaCl_2$). Another set of sections was pre-incubated in a series of alkaline solutions [pH 10.1–10.5 (0.1 increments); 24 mM $CaCl_2$, 53 mM glycine, 52 mM NaCl, 45 mM NaOH] for 10 min at 37 °C and rinsed for 3 min in deionized water (pH 8.5–9.0).

All sections were then incubated for 30 min in a freshly prepared ATP solution (pH 9.4; 20 mM sodium barbital, 14 mM $CaCl_2$, 2.5 mM ATP) at 37 °C. All sections were subsequently run through a series of 3 min rinses as follows: deionized water (pH 8.5–9.0), 2% calcium chloride, and 1% cobalt chloride, and stained for 3 min in 1% ammonium sulfide. Sections were then rinsed in cold running water for 5 min, dehydrated, and coverslipped with a xylene based mounting media. Fibers were classified as slow- or fast-twitch (fast-twitch classification was not specific as to the type of fast-twitch fiber and, therefore, included: IIA, fast-twitch oxidative glycolytic, IIX, fast-twitch intermediate oxidative glycolytic, and IIB, fast-twitch glycolytic) on the basis of basic and acidic pre-incubation protocols for myosin ATPase following the classification scheme of Hermanson and Evans (1993).

Digital images of stained sections were captured using a Zeiss AxioImager A1 microscope, a Zeiss AxioCam MRC Rev 3 color camera, and AxioVision v. 4.7 software (Zeiss North America, Thornwood, NY, USA) on an Intel Pentium D computer. For each *Phocoena* muscle sample, multiple images were taken from identical regions of each treatment (myosin ATPase acid and alkaline pre-incubations) described earlier. In comparison, for each *Tursiops* sample, images were taken from acidic treatments only.

Using the images of the sections stained for myosin ATPase activity after acidic pre-incubation, the minor axis (fiber diameter) of 30 fibers of each fiber-type (split between two images) was measured using ImageJ (v. 1.43u, with the setting "Fit Ellipse"). The entire set of either acidic (*Tursiops*) or alkaline (*Phocoena*) images for each muscle sample was printed for analysis (average set = 5 images). Printed images were analyzed to obtain fiber-type

percentages by number. The number of each type of fiber on each image was counted until a minimum of 300 fibers (*Phocoena* average: 1900 fibers; *Tursiops* average: 1400 fibers) were counted. For each image, the number of each type of fiber was divided by the total number of fibers counted and multiplied by 100% to express fiber number as a percentage of the total number of fibers. Using all analyzed images, average percentages (±1 SD) of fast-twitch fibers were then calculated for each muscle sample and these values were used to determine overall average (±1 SE) fast-twitch percentages for the muscles from each species.

Myosin heavy chain electrophoresis

Samples (approximately 2.5 mg) of each dolphin and porpoise vocal muscle, along with adult rat diaphragm, were minced and their myosin extracted for 60 min in a urea/thiourea gel sample buffer (8.0 M urea, 2.0 M thiourea, 0.08 M dithiothreitol, 0.04 M Trizma base, 0.12 M SDS, 0.004% bromophenol blue, pH 6.8) at 0 °C. The extracts were centrifuged at 13,000 rpm for 45 min at room temperature in an Eppendorf 5415D centrifuge (Eppendorf South Pacific Pty. Ltd., NSW, Australia). The supernatants were collected and heated at 100 °C for 2 min, cooled on ice for 5 min, and then stored at −20 °C.

Electrophoresis was performed in 8% acrylamide, 30% (v/v) glycerol separating gels, 4% acrylamide, and 5% (v/v) glycerol stacking gels. Aliquots (3–20 mL) of each vocal muscle and rat diaphragm myosin extract were electrophoresed at 75 V for 2 h, followed by 275 V for 24 h at 10 °C. Adult rat diaphragm was run alongside all cetacean samples as a control, because it expresses all three fast myosin isoforms (IIA, IIX, and IIB) and the slow isoform (I) (LaFramboise et al. 1991). Inclusion of this muscle in each gel enabled direct comparisons with the myosin isoforms expressed by cetacean samples. The separating gels were then silver stained following the protocol of Dearolf (2003), and digital images of the stained gels were captured using a Kodak Electrophoresis Documentation and Analysis System (EDAS) 290 consisting of a Kodak DC290 zoom digital camera and EDAS 290 LE Image Analysis Software (Kodak, Rochester, NY, USA).

Statistical analyses

All statistical analyses were run using the statistical programming software R (R version 3.2.0). A linear mixed-effects model, using the lme function from the nlme package, was used to test for differences in vocal muscle (RNM, LNM, PPS, and GGC) [Mb] by species, muscle type, and their interaction, while including specimen as a random effect. Subsequently, differences between the [Mb] of specific vocal muscles were examined separately by species using specified contrasts within the framework of the mixed-effects model using the contrast package (Kuhn et al. 2013). Separate linear mixed-effects models were used to test for differences in vocal muscle β and fiber-type profiles (% type II) by species, muscle type, and their interaction, while including specimen as a random effect. Small sample sizes precluded the performance of specific contrasts on β and fiber-type profile datasets. Fiber diameters of vocal muscles for each species were compared using separate linear mixed-effects models. In both models, muscle and fiber-type (slow- and fast-twitch) were included as fixed-effects, the interaction between muscle and fiber-type was tested, and specimen was included as a random effect. Given that we were only able to collect two locomotor muscle samples for *Phocoena* and none for *Tursiops*, we excluded locomotor muscle data from all statistical analyses. We did, however, include the locomotor data from *Phocoena* (this study) along with previously published values of *Tursiops* skeletal muscles in figures and tables as reference. For all analyses, statistical differences between values were accepted for $p < 0.05$.

Results

Biochemical analyses

The vocal musculature of *Phocoena* contained a higher [Mb] than *Tursiops* (mixed-effects model: $F_{1,7} = 15.43$, $p < 0.01$), with a marginal effect of muscle group (mixed-effects model: $F_{3,15} = 3.11$, $p = 0.058$), and no interaction effect. Specified contrasts revealed significant differences in [Mb] between vocal muscle groups in *Tursiops*, which included differences between the RNM and LNM ($t = -2.52$, $df = 20$, $p = 0.02$), the PPS and RNM ($t = -3.17$, $df = 20$, $p = 0.005$), the LNM and GGC ($t = 2.16$, $df = 20$, $p = 0.04$), and the PPS and GGC ($t = 2.76$, $df = 20$, $p = 0.01$). In *Tursiops*, the PPS exhibited the highest [Mb], while the RNM exhibited the lowest, although there was not a statistical difference in [Mb] between the RNM and the GGC. In *Phocoena*, there were no significant differences in [Mb] found between individual vocal muscles. However, there was a notable difference in [Mb] between all vocal muscles and the locomotor muscle samples examined (Fig. 2).

In regards to acid buffering capacity due to non-bicarbonate buffers, there was no effect of species (mixed-effects model: $F_{1,7} = 0.0005$, $p = 0.98$) and there was a significant effect of muscle group ($F_{3,14} = 4.19$, $p = 0.03$) and no interaction effect. For both *Tursiops* and *Phocoena*, the GGC had the highest muscle acid buffering capacity of all vocal muscles (Table 2). In *Tursiops*, the

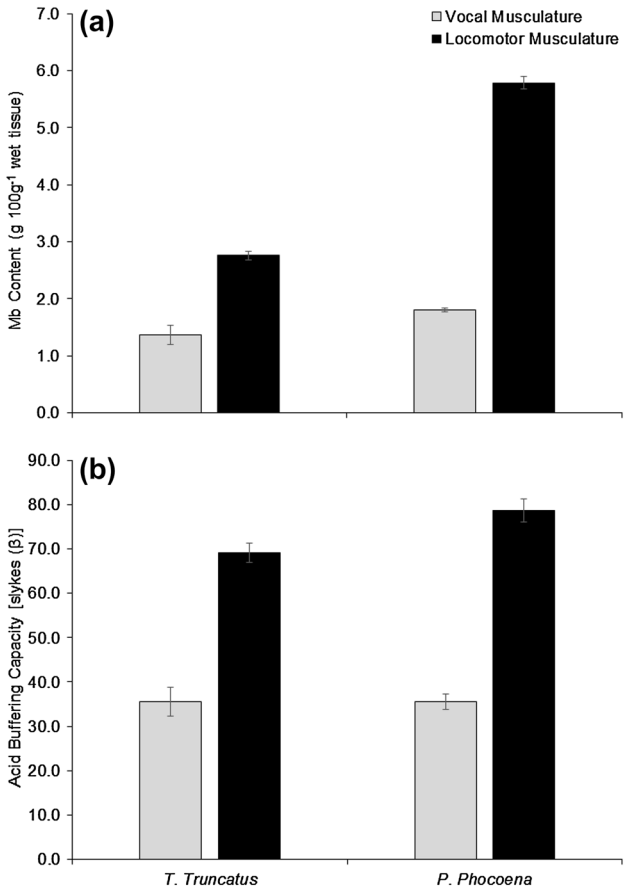

Fig. 2 Comparison of average (±SE) myoglobin content (**a**) and acid buffering capacity (**b**) between vocal (all muscles pooled) and locomotor (longissimus dorsi) muscles in *Tursiops* and *Phocoena*. All values were taken from this study with the exception of *Tursiops* locomotor muscle values which were adapted from Noren et al. (2001) and Noren (2004) for [Mb] and acid buffering values, respectively. All comparisons are significant ($p < 0.05$)

RNM exhibited the lowest acid buffering capacity. In general, regardless of the vocal muscle group, vocal musculature had approximately half of the buffering capacity of locomotor musculature (Fig. 2).

Muscle histochemistry

There were significant differences in vocal muscle fiber-type profiles (% type II, fast-twitch fibers) both by species (mixed-effects model: $F_{1,6} = 8.17$, $p = 0.03$) and muscle group ($F_{3,14} = 45.47$, $p < 0.0001$), but no interaction effect. In general, *Phocoena* vocal musculature had more fast-twitch fibers than *Tursiops* vocal musculature. There were notable differences observed in the fiber-type profiles of *Tursiops* vocal musculature (Table 3; Fig. 3), with the GGC exhibiting the highest percentage of fast-twitch fibers (79.7%) and the PPS exhibiting the lowest percentage (24.3%). Differences were also apparent across *Phocoena* vocal muscle groups (Table 4; Fig. 4), and those differences mirrored those observed for *Tursiops*. *Phocoena* GGC had the highest percentage of type II fibers (88.6%), while the PPS had the lowest (36.8%; Fig. 5).

In *Tursiops*, vocal muscle group had a significant effect on fiber size (mixed-effects model: $F_{3,22} = 7.20$, $p = 0.015$) and there was no effect of fiber-type ($F_{1,22} = 0.43$, $p = 0.51$), but there was an interaction effect ($F_{3,19} = 3.84$, $p = 0.02$). Overall, average diameters of vocal muscle fast-twitch (26.1 ± 5.0 µm) and slow-twitch (26.0 ± 4.4 µm) fibers were nearly identical (Table 5). Fast- and slow-twitch fibers in all vocal muscles were notably smaller than previously published values for longissimus dorsi fast-twitch fibers (54.5 ± 2.9 µm; Dearolf et al. 2000). Similarly, the fast-twitch fibers of *Tursiops* diaphragm muscle had greater average diameters (39.2 ± 1.6 µm; Dearolf 2002) than the fast- and slow-twitch fibers of *Tursiops* vocal muscles. Of particular note, the average fiber diameter of *Tursiops* PPS (22.4 ± 1.81 µm) was significantly smaller than the average fiber diameters of all other vocal muscles (Fig. 6a).

In *Phocoena*, the fast- and slow-twitch fibers did not differ significantly in size (mixed-effects model: $F_{1,12} = 0.39$, $p = 0.54$) and there was no interaction between fiber-type and muscle; however, fiber diameters were significantly different by vocal muscles ($F_{3,12} = 3.96$, $p = 0.04$; Table 6). When averaging the diameters of fast- and slow-twitch muscle fibers within a single muscle, the average fiber diameter of *Phocoena*

Table 2 Average (±SE) myoglobin concentration (g Mb × 100 g wet tissue^{-1}) and non-bicarbonate buffering capacity (β) of bottlenose dolphin (*Tursiops truncatus*) and harbor porpoise (*Phocoena phocoena*) muscle samples

Muscle type	*Tursiops truncatus*		*Phocoena phocoena*	
	[Mb]	β	[Mb]	β
Right nasal musculature	1.07 ± 0.03 (4)	28.12 ± 1.99 (4)	1.74 ± 0.07 (4)	36.90 ± 2.84 (3)
Left nasal musculature	1.59 ± 0.18 (4)	32.39 ± 3.23 (4)	1.90 ± 0.07 (4)	30.10 ± 2.70 (4)
Palatopharyngeal sphincter	1.72 ± 0.29 (4)	39.22 ± 4.52 (4)	1.79 ± 0.14 (4)	33.91 ± 2.98 (4)
Genioglossus complex	1.11 ± 0.06 (3)	42.53 ± 4.16 (3)	1.80 ± 0.13 (3)	41.32 ± 2.95 (3)
Longissimus dorsi	2.76 ± 0.15[a]	69.10 ± 4.40[a]	5.79 ± 0.11 (2)	78.66 ± 2.54 (2)

Sample size is displayed in parentheses

[a]Logissimus dorsi [Mb] and β values from Noren et al. (2001) and Noren (2004), respectively

Table 3 Percentage of fast-twitch fibers (mean ± SD) by count in the right nasal musculature (RNM), left nasal musculature (LMN), palatopharygneal sphincter (PPS), and genioglossus complex (GGC), of the bottlenose dolphin (*Tursiops truncatus*) specimens from this study

Specimen ID	RNM	LNM	PPS	GGC
WAM628	60.2 ± 8.6	35.0 ± 6.5	25.0 ± 2.7	76.9 ± 6.4
SWT001	55.0 ± 6.1	30.0 ± 4.7	29.9 ± 2.5	–
KLC156	51.5 ± 4.7	59.5 ± 3.5	13.5 ± 3.7	77.6 ± 2.3
WAM650	55.0 ± 11.6	44.7 ± 9.7	28.6 ± 6.7	84.5 ± 2.3

An average of five images was taken from each muscle and analyzed to determine percentages of fast-twitch fibers and associated standard deviations. Specimen are listed in an order of decreasing standard body length

PPS (15.5 ± 1.8 µm) was significantly smaller than that of the LNM (23.9 ± 1.6 µm). However, all other muscle groups had fibers that were similar in average size (Fig. 6b).

Myosin heavy chain electrophoresis

All *Tursiops* muscles demonstrated three myosin isoforms subsequent to heavy chain electrophoresis (Fig. 7a). One of the bands migrated at the same rate as the type I, slow-twitch isoform in rat costal diaphragm described by LaFramboise et al. (1991). The other two myosin bands in *Tursiops* migrated differently than the myosin isoforms expressed in rat costal diaphragm. One of the *Tursiops* bands, identified as Fast 1, migrated more slowly than the rat fast-twitch type IIA and IIX isoforms (Schiaffino et al. 1990), while the remaining *Tursiops* band (+) migrated more quickly than the rat type I isoform (Fig. 7a). *Tursiops* RNM expressed more of the Fast 1 isoform (darker band) and less of the type I isoform in comparison to the expression of these isoforms in the LNM. In addition, *Tursiops* PPS expressed the type I isoform almost exclusively, while the GGC expressed more of the Fast 1 isoform (Fig. 7a). All of these myosin heavy chain expression patterns confirm the histochemical results from *Tursiops* vocal muscles

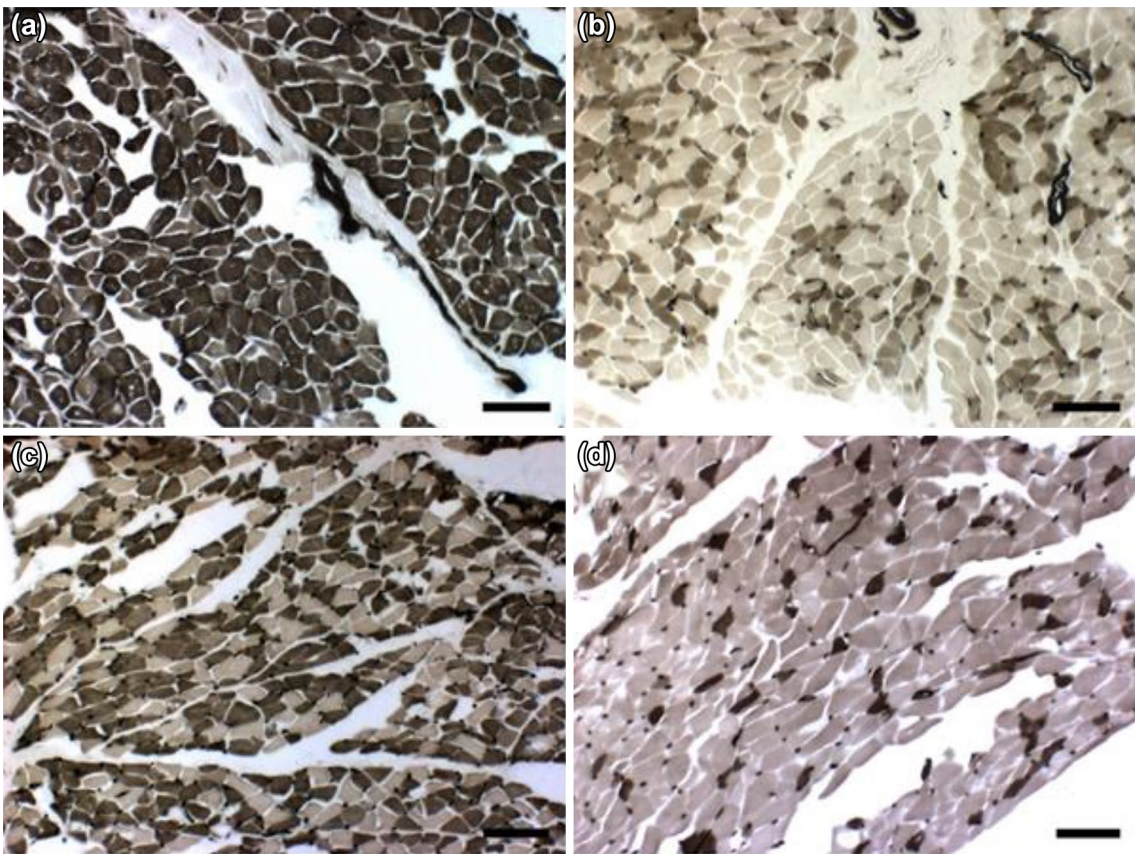

Fig. 3 Representative cross sections of the vocal muscles of **a, b** adult (WAM628) and **c, d** sub-adult (**c** SWT001; **d** WAM650) bottlenose dolphins stained for myosin ATPase activity after acidic pre-incubation. Vocal muscles are displayed in the following order: **a** left nasal musculature, **b** right nasal musculature, **c** palatopharyngeal sphincter, and **d** genioglossus complex. In all *panels*, slow-twitch fibers are stained dark and fast-twitch fibers are stained light. The *black scale bar* displayed in the *bottom right corner* of each image = 100 µm

Table 4 Percentage of fast-twitch fibers (mean ± SD) by count in the right nasal musculature (RNM), left nasal musculature (LNM), palatopharygneal sphincter (PPS), genioglossus complex (GGC), and longissimus dorsi (LD) of the harbor porpoise (*Phocoena phocoena*) specimens from this study

Specimen ID	RNM	LNM	PPS	GGC	LD
C464	56.0 ± 8.4	56.1 ± 10.0	–	–	–
CRC1475	–	56.6 ± 8.8	47.0 ± 1.7	88.6 ± 3.7	53.1 ± 4.6
SJC0025	32.4 ± 27.6	57.3 ± 4.6	23.1 ± 3.2	88.6 ± 5.1	63.1 ± 1.0
C458	53.9 ± 3.5	59.2 ± 10.1	40.3 ± 7.0	88.6 ± 4.4	–

An average of five images was taken from each muscle and analyzed to determine percentages of fast-twitch fibers and associated standard deviations. Specimen are listed in an order of decreasing standard body length

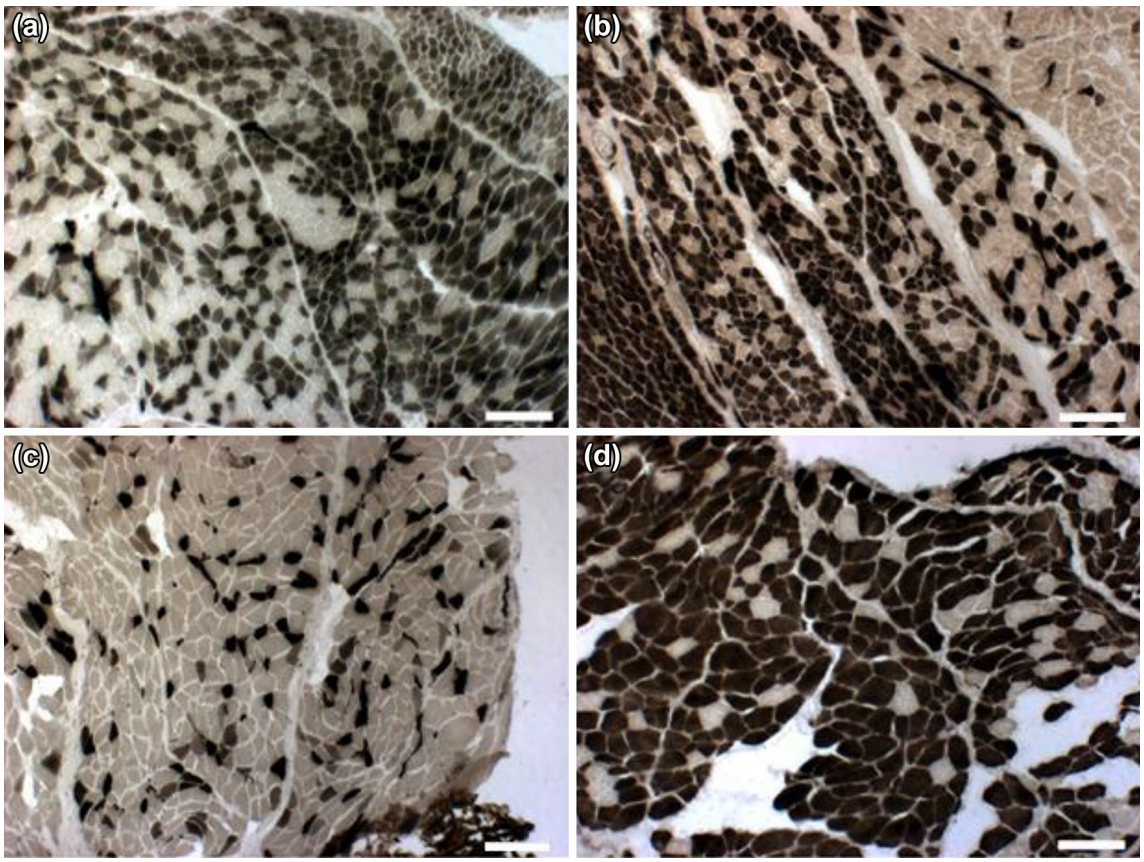

Fig. 4 Representative cross sections of the vocal muscles of **a, b** subadult (C458) and **c, d** adult (SJC0025) harbor porpoises stained for myosin ATPase activity after alkaline pre-incubation. Vocal muscles are displayed in the following order: **a** left nasal musculature, **b** right nasal musculature, **c** palatopharyngeal sphincter, and **d** genioglossus complex. In all *panels*, slow-twitch fibers are stained light and fast-twitch fibers are stained dark. The *white scale bar* displayed in the *bottom right corner* of each image = 100 µm

(Fig. 5). Of note, the expression of the + isoform varied across the four vocal muscles of the specimen (WAM628) used in Fig. 7a, with the LMN expressing the most (darker band), but the expression of this isoform in the vocal muscles of *Tursiops* varied across all individuals.

Phocoena muscles only demonstrated two myosin isoforms subsequent to heavy chain electrophoresis (Fig. 7b). Similar to *Tursiops*, one of the *Phocoena* bands migrated at the same rate as the rat type I isoform, and one migrated more slowly (Fast 2) than the rat fast types IIA and IIX isoforms. However, the Fast 2 band in the *Phocoena* muscle migrated more quickly than the Fast 1 in the *Tursiops* muscles (not shown), and none of the *Phocoena* muscles expressed the *Tursiops* + isoform (Fig. 7b). The *Phocoena* RNM expressed more of the type I isoform (darker band) than the Fast 2 isoform in comparison to the LNM (Fig. 7b). The PPS expressed more of the Fast 2 isoform and less of the type I isoform, but this muscle expressed

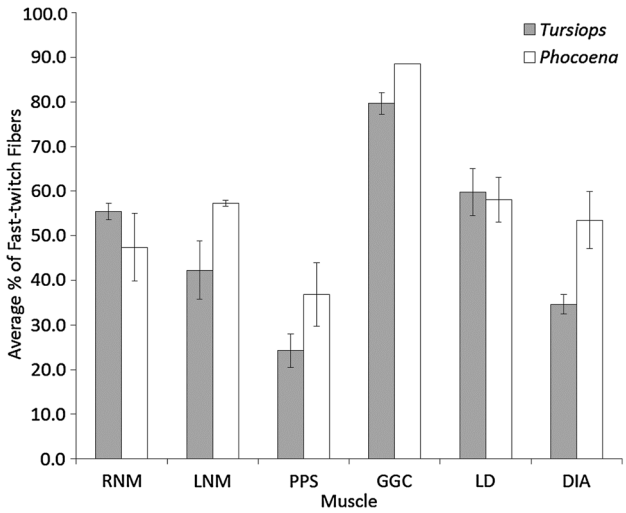

Fig. 5 Average percentages of fast-twitch fibers (±SE) by count in the right nasal musculature (RNM), left nasal musculature (LNM), palatopharyngeal sphincter (PPS), genioglossus complex (GGC), longissimus dorsi (LD), and diaphragm (DIA) of harbor porpoises (*Phocoena phocoena*) and bottlenose dolphins (*Tursiops truncatus*). All values were determined as part of this study with the exception of *Tursiops* LD (Dearolf et al. 2000), *Tursiops* DIA (Dearolf 2002), and *Phocoena* DIA (Dearolf unpublished data)

more of the type I isoform than the LMN or GGC. The GGC expressed more of the Fast 2 isoform and less of the type I isoform, while the longissimus dorsi expressed approximately equal amounts of both isoforms. In general, these expression patterns confirm that histochemical results described here for *Phocoena* vocal muscles (Fig. 5).

Discussion

Our results reveal shared biochemical and structural traits of vocal musculature across *Tursiops* and *Phocoena*. Broadly, the [Mb] and non-bicarbonate buffering capacity of vocal muscles are less than half of values defined for locomotor muscles of the same species. In addition, vocal muscles have smaller muscle fibers than those found in locomotor muscles and (excluding the GGC) contain a lower percentage of type II, fast-twitch fibers (Fig. 8). Combined, these physiological characteristics support recent studies highlighting the relatively low cost of sound production in comparison to locomotion in *Tursiops* (Williams 1999; Noren et al. 2013; Holt et al. 2015); a finding that is likely true across odontocete species (Dunkin et al. in prep). Although vocal muscles share many of the same physiological properties, which deviate in distinctive ways from previously described properties of locomotor and ventilatory muscles (Fig. 8), we identified a number of differences between vocal muscle groups, as well as interspecies differences, which provide valuable insight into the functioning of these muscles both within and across species.

Biochemical and morphological characteristics

The PPS, which is known for pressurizing air spaces within the head (Dormer 1979; Huggenberger et al. 2008, 2009; Cranford et al. 2011), exhibited the lowest percentage of type II fibers (Fig. 5). The prevalence of type I, slow-twitch fibers in the PPS of both species was revealed through fiber-type analyses; although myosin heavy chain analyses only confirmed these results for *Tursiops* (Fig. 7). The high percentage of type I fibers that make up the PPS in each species (75.7% in *Tursiops*; 63.2% in *Phocoena*) indicates a heavy reliance on aerobic metabolism in this muscle; a characteristic common of sphincter muscles that must hold contractions for extended periods of time (Schrøder and Reske-Nielsen 1983; Mu and Sanders 2002). These values are similar to the percentage of slow-twitch muscle defined for *Tursiops* diaphragm (66%; Dearolf 2003); however, *Tursiops* PPS displayed the highest percentage of slow-twitch fibers by count that has been reported for any muscle in this species to date (Fig. 8). Interestingly, the *Tursiops* PPS had the highest [Mb] and second β of all vocal muscles examined for that species. Given these physiological properties, the PPS appears to be a relatively active muscle that relies heavily

Table 5 Diameters (microns) of type I (slow-twitch) and type II (fast-twitch) fibers (mean ± SD) in the right nasal musculature (RNM), left nasal musculature (LMN), palatopharygneal sphincter (PPS), and genioglossus complex (GGC) of the bottlenose dolphin (*Tursiops truncatus*) specimens from this study

Specimen ID	RNM		LNM		PPS		GGC	
	Type I	Type II	Type I	Type II	Type I	Type II	Type I	Type II
WAM628	25.0 ± 6.0	26.7 ± 4.8	34.1 ± 5.8	23.8 ± 3.8	23.7 ± 5.2	23.1 ± 5.7	28.0 ± 6.3	31.2 ± 8.9
SWT001	22.7 ± 3.3	23.5 ± 5.4	35.2 ± 7.6	26.9 ± 6.5	23.7 ± 4.7	24.1 ± 4.6	–	–
KLC156	25.7 ± 5.1	30.0 ± 5.2	27.3 ± 5.9	22.9 ± 4.5	22.0 ± 3.5	19.5 ± 4.7	28.2 ± 7.8	39.8 ± 9.5
WAM650	24.0 ± 4.8	21.0 ± 4.0	28.9 ± 4.7	27.7 ± 4.0	20.1 ± 4.8	23.0 ± 3.2	21.2 ± 4.1	27.6 ± 6.2

Specimen are listed in an order of decreasing standard body length

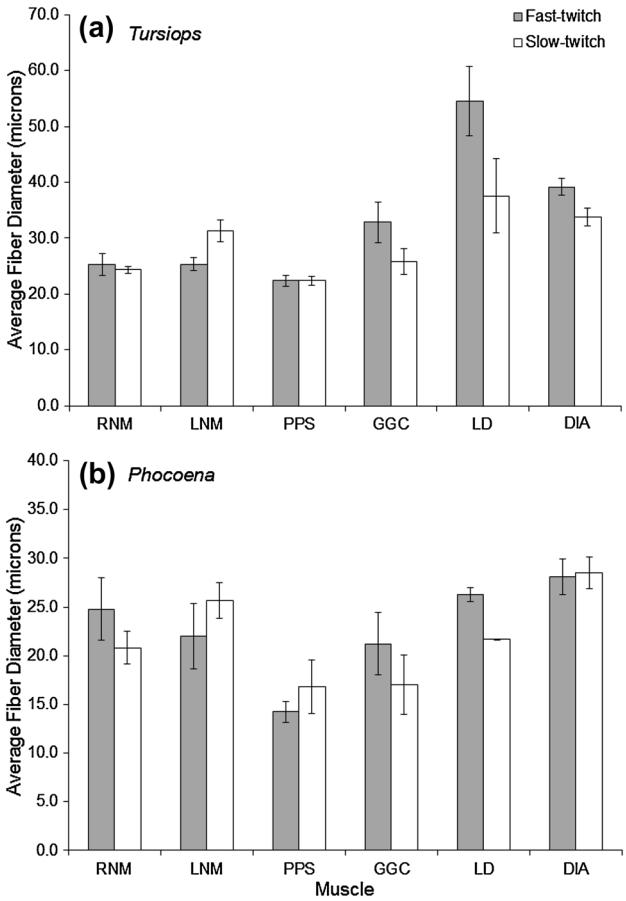

Fig. 6 Average diameters (microns) of fast-twitch and slow-twitch fibers (±SE) of **a** bottlenose dolphin (*Tursiops truncatus*) and **b** harbor porpoise (*Phocoena phocoena*) right nasal musculature (RMN), left nasal musculature (LNM), palatopharyngeal sphincter (PPS), genioglossus complex (GGC), longissimus dorsi (LD), and diaphragm (DIA). All values were determined as part of this study with the exception of *Tursiops* LD (Dearolf et al. 2000), *Tursiops* DIA (Dearolf 2002), and *Phocoena* DIA (Dearolf unpublished data)

on aerobic metabolism, but has the capacity to manage the buildup of anaerobic by-products when necessary. In contrast, [Mb] and β values were fairly comparable across all vocal muscles examined for *Phocoena*.

The GGC exhibited the highest percentage of type II fibers of any muscle examined in both *Phocoena* (88.6% type II) and *Tursiops* (79.7% type II), including the longissimus dorsi (*Phocoena*: current study, *Tursiops*: Kielhorn et al. 2013). This prevalence of fast-twitch fibers in the GGC of both species was also revealed by the increased expression of the Fast 2 (*Phocoena*) and Fast 1 (*Tursiops*) myosin heavy chain isoforms in these muscles. The only muscle that has been found to have a similarly predominant fast-twitch fiber-type profile is the *Tursiops* sternohyoid muscle (Fig. 8; Cotten et al. 2008). Given that the sternohyoid is positioned in the same region of the head as the muscles that make up the GGC (genioglossus, hyoglossus, and styloglossus) and may share some of the same functional roles, the similarity in fiber profiles between these muscles was not unexpected.

Both the GGC and the sternohyoid serve dual roles (Fig. 8): the GGC functions in both sound production and feeding, while the sternohyoid functions in both ventilation and feeding (Lawrence and Schevill 1956; Liste et al. 2006; Werth 2007; Huggenberger et al. 2008, 2009; Cotten et al. 2008). The need for rapid muscle contraction during both sound production and ventilation likely drives the high proportion of fast-twitch muscle fibers in each of these muscles. In addition to a predominately fast-twitch muscle fiber-type profile, the GGC had the highest β of any vocal muscle in both *Phocoena* and *Tursiops* (Table 2). Together, these results indicate frequent use of fast-twitch muscle contractions and anaerobic metabolism, as well as the ability to buffer against anaerobic waste products.

The RNM and LNM shared many characteristics across species, including a fairly even mix of type I and type II fibers and comparable fiber diameters. Interestingly, staining the RNM and LNM for their myosin ATPase activities revealed defined boundaries within the same muscle sample that delineated areas composed mainly of type I and areas mainly composed of type II fibers (Figs. 3a, b, 4a, b). Because right and left nasal muscle samples were composed of five distinct muscles (posterior externus, anterior externus, posterior internus, anterior internus, and

Table 6 Diameters (microns) of type I (slow-twitch) and type II (fast-twitch) fibers (mean ± SD) in the right nasal musculature (RNM), left nasal musculature (LMN), palatopharygneal sphincter (PPS), genioglossus complex (GGC), and longissimus dorsi (LD) of the harbor porpoise (*Phocoena phocoena*) specimens from this study

Specimen ID	RNM		LNM		PPS		GGC		LD	
	Type I	Type II	Type I	Type II	Type I	Type II	Type I	Type II	Type I	Type II
C464	21.5 ± 4.9	30.8 ± 6.7	28.7 ± 10.6	31.5 ± 6.5	–	–	–	–	–	–
CRC1475	–	–	21.9 ± 4.7	15.9 ± 4.2	19.9 ± 6.0	14.9 ± 5.3	16.0 ± 3.9	20.1 ± 6.8	21.7 ± 4.6	27.0 ± 6.6
SJC0025	23.4 ± 6.2	19.7 ± 7.1	28.9 ± 8.7	20.2 ± 7.5	19.2 ± 4.6	15.7 ± 3.8	22.7 ± 5.6	27.3 ± 5.6	21.6 ± 4.6	25.6 ± 4.7
C458	17.6 ± 4.5	23.9 ± 7.1	23.2 ± 4.3	20.5 ± 3.1	11.3 ± 3.1	12.1 ± 2.5	12.3 ± 3.1	16.3 ± 5.4	–	–

Specimen are listed in an order of decreasing standard body length

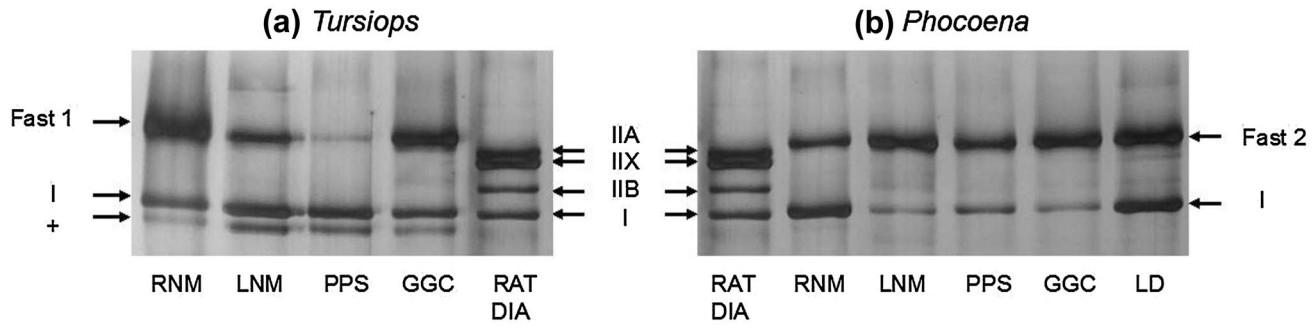

Fig. 7 Eight percent SDS–PAGE of myosin heavy chains from the diaphragm of a rat (RAT DIA), the vocal muscles (*RNM* right nasal musculature, *LNM* left nasal musculature, *PPS* palatopharyngeal sphincter, *GGC* genioglossus complex) of **a** an adult (WAM628) bottlenose dolphin (*Tursiops truncatus*) and **b** a sub-adult (C458) harbor porpoise (*Phocoena phocoena*), and the locomotor (LD) muscle of an adult (CRC1475) harbor porpoise. The four myosin heavy chains labeled in the rat diaphragm (see LaFramboise et al. 1991) are shown for comparison with the **a** *Tursiops* and **b** *Phocoena* samples. **a** *Tursiops* vocal muscle samples have only one myosin isoform that comigrates with an isoform of the rat diaphragm (type I), and they differ in the level of expression of this isoform. The LNM and PPS express more of this isoform than the other two muscles. Dolphins also express two isoforms that do not comigrate with the isoforms found in the rat diaphragm (labeled Fast 1 and +). The RNM and GGC express more of the Fast 1 isoform, while the LNM and PPS express more of the +. **b** *Phocoena* vocal muscle samples also have only one isoform that comigrates with an isoform of the rat (type I). The RNM and LD show similar levels of expression of this isoform, the PPS expresses slightly less, and the LNM and GGC express very little type I myosin. Porpoises also express one isoform that does not comigrate with the isoforms found in rat diaphragm (labeled Fast 2) or the Fast 1 isoform in the dolphin muscles (not shown). The LNM, GGC, and LD show similar levels of this isoform, while the PPS expresses slightly less, and the RNM expresses the lowest amount of Fast 2

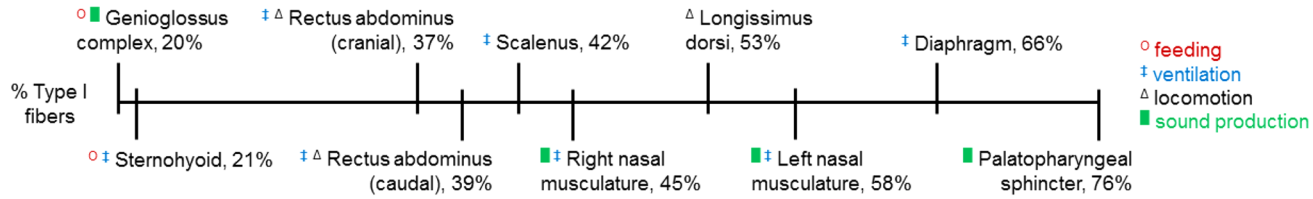

Fig. 8 Relative percentage of type I (slow-twitch) fibers by count in various *Tursiops* skeletal muscles. *Colored symbols* denote the main function(s) of each skeletal muscle or muscle group: *circle* feeding (*red*), *dagger* ventilation (*blue*), *triangle* locomotion (*black*), and *rectangle* sound production (*green*). Values for the genioglossus complex, right and left nasal musculature, and palatopharyngeal sphincter were determined in this study. Values for all other muscles were adapted from previously published studies [sternohyoid, rectus abdominus, and scalenus (Cotten et al. 2008); longissimus dorsi (Kielhorn et al. 2013); diaphragm (Dearolf 2003)]. (Color figure online)

the intermedius) which were all fan-shaped, highly overlapping and interconnected, we propose that although the RNM and LNM were found to have an even mix of type I and type II fibers, that the individual muscles that make up the RNM and LNM likely have very distinct fiber-type profiles; which combined, allow for fine scale control of air movement within the head, sound production, and sound modification.

A number of studies have examined the oxygen storage capacity, specifically [Mb], of *Phocoena* locomotor muscle. Adult *Phocoena* [Mb] has been reported to be as low as 2.56 g Mb × 100 g wet tissue^{-1} and as high as 4.10 g Mb × 100 g wet tissue^{-1} (Blessing 1972; Noren and Williams 2000; Noren et al. 2014). Our locomotor muscle data revealed a higher [Mb] for the two individuals examined in this study (5.79 g Mb × 100 g wet tissue^{-1}), which was more comparable to values determined for other small odontocetes such as spinner dolphins (5.5 g Mb × 100 g wet tissue^{-1}) and pygmy killer whales (5.7 g Mb × 100 g wet tissue^{-1}) (Dolar et al. 1999). Although the [Mb] of our *Phocoena* locomotor muscle was not as high as some of the most impressive small odontocetes, which can have [Mb] greater than 6 g Mb × 100 g wet tissue^{-1} (Fraser's dolphin, Dolar et al. 1999; false killer whale, Harrison and Davis 1998). There are a number of reasons as to why our specimens may have exhibited higher [Mb] than the previous studies, but our values fall within a reasonable range of variability. Indeed, within-species variability in oxygen storage capacity can be driven by a variety of factors including, but not limited to, diving patterns, physiological state, and seasonal changes in prey distribution; specifically, [Mb] can vary considerably between individuals of the same

species (Weise and Costa 2007; Villegas-Amtmann and Costa 2010; Villegas-Amtmann et al. 2012; Hückstädt et al. 2016).

Although our [Mb] values for *Phocoena* locomotor muscle were higher than the previous estimates, the results of our non-bicarbonate acid buffering analyses of *Phocoena* locomotor muscle were nearly identical to previously reported values (78.7 ± 2.54 β, this study; 78.5 ± 5.5 β, Noren et al. 2014), and were more than double the β found for any *Phocoena* vocal muscle. In addition, this was the first study to provide fiber-type profile data for any *Phocoena* muscle, including the longissimus dorsi. In terms of fiber-type profile, the *Phocoena* longissimus dorsi had a comparable percentage of type II fibers (58.1%) to *Tursiops* (53.3%; Kielhorn et al. 2013). There was marked variability between the fiber-type profile of *Phocoena* vocal muscles and the longissimus dorsi; this was true of *Tursiops*, as well (Fig. 8). In both species, the greatest percentage of type II fibers was found in the GGC and the smallest percentage was found in the PPS, highlighting the very different ways in which specific vocal muscles work in unison to aid in sound production.

Linking structure and function

In cetaceans, the GGC is responsible for moving air into nasal cavities and recycling air during sound production (Lawrence and Schevill 1956; Huggenberger et al. 2008). Thus, this muscle group must be capable of fast and forceful contractions to move air through the PPS and into nasal cavities; which necessitates a dominance of fast-twitch fibers. Indeed, in a variety of taxa, sound production muscles generally have a higher proportion of fast-twitch fibers and other specialized physiological features to increase contractile properties (Rome et al. 1996).

A high prevalence of fast-twitch oxidative glycolytic (FOG) fibers has been identified in the vocal muscles of male *Xenopus laevis* and *Hyla versicolor*, two species of frog known for long duration mating vocalizations that result from rapid and sustained contraction of calling muscles (Marsh and Taigen 1987; Sassoon et al. 1987). Although we were unable to test for the existence of FOG fibers in this study, given its role in sound production, we would expect a predominance of FOG fibers in the GGC of cetaceans. Similarly, it would be interesting to determine if any cetacean vocal muscles display superfast muscle kinematics as has been described in the sound producing muscles of some fish, songbird, and bat species (Rome 2006; Elemans et al. 2008, 2011). It is important to note that the GGC also serves as a major feeding muscle in cetaceans (Werth 2007; Fig. 8); and it has been well established in rats and humans that skeletal muscles associated with feeding tend to have a predominance of type II, fast-twitch fibers (Smith 1989; Petrof et al. 1992; Sutlive et al. 1999, 2000; Saigusa et al. 2001; Liu et al. 2009). Thus, the dual role of the GGC in cetacean sound production and feeding has likely driven the prevalence of fast-twitch fibers found in the GGC of both *Tursiops* and *Phocoena*.

While there were many similarities between the RNM and LNM within and across species, the documented differences in key characteristics of these muscles by species appear to mirror differences in the species-specific functionality of these muscles. It has widely been shown that *Tursiops* are capable of producing complex sounds, including both broadband clicks and tonal whistles, which they can perform at the same time (Madsen et al. 2013; Ridgway et al. 2015); while *Phocoena* are only capable of producing narrower band higher frequency clicks (Au et al. 2006; Madsen et al. 2010). Of note is that clicks originate from the right side of the head and whistles originate from the left in *Tursiops* (Mead 1975; Dormer 1979; Madsen et al. 2013). In addition, asymmetrical cranial morphology (e.g., differences in the size of the nasal air sacs on either side of the head) has been documented in *Tursiops* (Dormer 1979).

Our results show that for *Tursiops*, the LNM had the second highest [Mb] of all vocal muscles, while the RNM had the lowest. However, both left and right nasal musculature had relatively low buffering capacity. In addition, compared to *Tursiops* locomotor muscle, LNM had a much higher proportion of type I fibers. These data indicate a reliance on aerobic metabolism and support the findings that in *Tursiops*, whistles are more energetically expensive than clicks. Indeed, the cost of clicking has been found to be negligible (Noren et al. in prep). Whistle production requires a significantly higher nasal cavity pressure than echolocation click production of a similar amplitude (Ridgway et al. 2001), which may drive the higher cost of whistles if the muscles that support these sounds must work more intensely to promote high pressure and quick air movement within the head (Holt et al. 2015).

It should be noted that while a significantly higher nasal cavity pressure is required for whistle production, pressurization of the air spaces occurs from contraction of muscles on both sides of the head during sound production, even when only one set of phonic lips is being used to produce sound (Ridgway et al. 1980). Metering pressurized air within the bony nares past the nasal plug and through the phonic lips produces sound, while modifying the shape of the phonic lips (through the action of nasal complex muscles, including those within the LNM and RNM) is believed to dictate the sound type, as well as sound modification in both amplitude and frequency (Cranford et al. 1996; Huggenberger et al. 2009). When on a breath-hold, spent air in the vestibular sacs can be recycling back down by withdrawal of the nasal plug via relaxation of skeletal muscles within and around the nasal complex (Dormer

1979; Amundin and Andersen 1983). The higher [Mb] and prevalence of type I fibers in the LNM compared to the RNM, a result supported by the myosin heavy chain electrophoretic analyses, agree with the proposed relative functions and associated functional and metabolic demands of each of these sets of muscles (whistling on the left, clicking on the right) within *Tursiops*. In *Phocoena*, a species which does not whistle (Au et al. 2006; Madsen et al. 2010), differences between the RNM and LNM were not significant.

Interestingly, although the fiber-type profiles of the RNM and LNM of *Phocoena* were not significantly different, the LNM did contain a greater proportion of fast-twitch fibers; a pattern that was opposite to that which was identified in *Tursiops* (Fig. 5). The difference in the construction of the two muscles in *Phocoena* was also reflected in their myosin heavy chain expression. The LNM expressed more of the Fast 2 isoform and less of the type I, in comparison to the RNM. This difference in fiber-type profile and myosin expression between the two suggests that these muscles may play different roles during vocalizations in *Phocoena*, but since these cetaceans only click (Au et al. 2006; Madsen et al. 2010), it is currently unknown why there is a difference in the construction of the RNM and LNM in this species.

In addition to the difference in the construction of the *Phocoena* RNM and LNM, the myosin heavy chain analyses demonstrated that the PPS in this cetacean expressed more of the Fast 2 isoform and less of the type I, a result that does not support the fiber-type profile data. However, as mentioned above, all of the studied muscles exhibited regional variability in fiber-type profiles, and of the *Phocoena* PPS muscles studied, C458 had the highest variability (7%) in fiber-type profile. This variability was also reflected in the heavy chain gel analyses of C458, which was our only sub-adult specimen (Fig. 7b). Because other muscles with a sphincter function, like the esophageal region of the diaphragm, gain slow-twitch fibers as individuals get older (Cobb et al. 1994), the myosin expression in the PPS of C458 may reflect an immature condition, although we would expect the developmental period for this muscle to have occurred, while this animal was a dependent calf. There is some support that the PPS of C458 may have still been developing, given the primarily slow-twitch profile (76.9% type I) of the PPS of one of our adult *Phocoena* (SJC0025), but given our small sample size which we cannot rule out individual variation.

Conclusion

This study highlights the unique physiological characteristics of individual vocal muscles that support sound production in odontocetes and provides insight into the specialized roles of each vocal muscle. Overall, individual muscles share similar physiological characteristics, regardless of species, that are indicative of their functional role in sound production. Indeed, the PPS is a highly aerobic, predominately slow-twitch muscle, which aids in its ability to maintain intracranial pressure in both *Tursiops* and *Phocoena*. The GGC contains a disproportionate number of fast-twitch fibers, which likely aids in its ability to move air against high pressure gradients within the head. Most notably, there are within and between species differences between the RNM and LNM, and these differences appear reflective of the vocal capabilities and repertoires of each species. Ultimately, these data reveal detailed physiological properties of vocal muscles which enhance our current understanding of odontocete sound production.

Acknowledgements We thank Joy Reidenberg, Ted Cranford, Bill McLellan, Ann Pabst, Mario Muscedere, Sarah McHugh, Megan Murphy, and Adrienne White, as well as the Long Marine Lab Marine Mammal Stranding Network, the Marine Mammal Center, the UNCW Stranding Network, and the Southwest Fisheries Science Center. This research was conducted under NMFS Scientific Research Permit #19590 to TMW, and NOAA Parts Authorization 110314 to RCD.

Compliance with ethical standards

Funding This research was supported by the Office of Naval Research (N000141410460 to TMW and RCD; and N0001416IP00023, N0001415IP00039, and N0001414IP20045 to DPN and MMH).

Conflict of interest The authors declare no conflict of interest.

Ethical approval This article does not contain any studies with live animals performed by any of the authors.

References

Amundin M, Andersen SH (1983) Bony nares air pressure and nasal plug muscle activity during click production in the harbour porpoise, Phocoena phocoena, and the bottlenosed dolphin, *Tursiops truncatus*. J Exp Biol 105:275–282

Au WWL, Kastelein RA, Benoit-Bird KJ et al (2006) Acoustic radiation from the head of echolocating harbor porpoises (*Phocoena phocoena*). J Exp Biol 209:2726–2733. doi:10.1242/jeb.02306

Blessing MH (1972) Studies on the concentration of myoglobin in the sea-cow and porpoise. Comp Biochem Physiol Part A 41:475–480. doi:10.1016/0300-9629(72)90005-9

Bradbury JW, Vehrencamp SL (1998) Sound production. Princ. Anim. Commun. Sinauer Associates, Inc., Sunderland, pp 75–112

Burns JM, Castellini MA (1996) Physiological and behavioral determinants of the aerobic dive limit in Weddell seal (*Leptonychotes weddellii*) Pups. J Comp Physiol B 166:473–483. doi:10.1007/BF02338290

Cartwright R, Newton C, West KM et al (2016) Tracking the development of muscular myoglobin stores in mysticete calves. PLoS One 11:1–18. doi:10.1371/journal.pone.0145893

Castellini MA, Somero GN (1981) Buffering capacity of vertebrate muscle: correlations with potentials for anaerobic function. J Comp Physiol B 143:191–198

Castellini MA, Kooyman GL, Ponganis PJ (1992) Metabolic rates of freely diving Weddell seals: correlations with oxygen stores, swim velocity and diving duration. J Exp Biol 165:181–194

Cobb MA, Schutt WA, Petrie JL, Hermanson JW (1994) Neonatal development of the diaphragm of the horse, *Equus caballus*. Anat Rec 238:311–316

Cotten PB, Piscitelli MA, McLellan WA et al (2008) The gross morphology and histochemistry of respiratory muscles in bottlenose dolphins, *Tursiops truncatus*. J Morphol 269:1520–1538. doi:10.1002/jmor.10668

Cranford TW, Amundin M, Norris KS (1996) Functional morphology and homology in the odontocete nasal complex: implications for sound generation. J Morphol 228:223–285. doi:10.1002/(SICI)1097-4687(199606)228:3<223::AID-JMOR1>3.0.CO;2-3

Cranford TW, Elsberry WR, Van Bonn WG et al (2011) Observation and analysis of sonar signal generation in the bottlenose dolphin (*Tursiops truncatus*): evidence for two sonar sources. J Exp Mar Bio Ecol 407:81–96. doi:10.1016/j.jembe.2011.07.010

Dearolf JL (2002) Morphology and development of the diaphragm of bottlenose dolphins (*Tursiops trunatus*). Cornell University, Ithaca

Dearolf JL (2003) Diaphragm muscle development in bottlenose dolphins (*Tursiops truncatus*). J Morphol 256:79–88. doi:10.1002/jmor.10077

Dearolf JL, McLellan WA, Dillaman RM et al (2000) Precocial development of axial locomotor muscle in bottlenose dolphins (*Tursiops truncatus*). J Morphol 244:203–215. doi:10.1002/(SICI)1097-4687(200006)244:3<203::AID-JMOR5>3.0.CO;2-V

Dolar MLL, Suarez P, Ponganis PJ, Kooyman GL (1999) Myoglobin in pelagic small cetaceans. J Exp Biol 202:227–236

Dormer KJ (1979) Mechanism of sound production and air recycling in delphinids: cineradiographic evidence. J Acoust Soc Am 65:229–239. doi:10.1121/1.382240

Elemans CPH, Mead AF, Rome LC, Goller F (2008) Superfast vocal muscles control song production in songbirds. PLoS One 3:6–11. doi:10.1371/journal.pone.0002581

Elemans CPH, Mead AF, Jakobsen L, Ratcliffe JM (2011) Superfast muscles set maximum call rate in echolocating bats. Science 333:1885–1888. doi:10.1126/science.1207309

Gillooly JF, Ophir AG (2010) The energetic basis of acoustic communication. Proc R Soc B 277:1325–1331. doi:10.1098/rspb.2009.2134

Green RF, Ridgway SH, Evans WE (1980) Functional and descriptive anatomy of the bottlenosed dolphin nasolaryngeal system with special reference to the musculature associated with sound production. Anim. Sonar Syst. Springer US, pp 199–228

Harrison LK, Davis RW (1998) Heterogeneity of myoglobin in cetacean swimming muscles. In: The world marine mammal science conference, Monaco, 20–24 January 1998, p 60

Hermanson J, Evans H (1993) The muscular system. Miller's Anat. Dog. W.B. Saunders, Philadelphia, pp 258–384

Hermanson JW, Hurley KJ (1990) Architectural and histochemical analysis of the biceps brachii muscle of the horse. Acta Anat (Basel) 137:146–156. doi:10.1017/CBO9781107415324.004

Hildebrand JA (2009) Anthropogenic and natural sources of ambient noise in the ocean. Mar Ecol Prog Ser 395:5–20. doi:10.3354/meps08353

Holt MM, Noren DP, Dunkin RC, Williams TM (2015) Vocal performance affects metabolic rate in dolphins: implications for animals communicating in noisy environments. J Exp Biol 2:1–8. doi:10.1242/jeb.122424

Houser DS, Finneran J, Carder D et al (2004) Structural and functional imaging of bottlenose dolphin (*Tursiops truncatus*) cranial anatomy. J Exp Biol 207:3657–3665. doi:10.1242/jeb.01207

Hückstädt LA, Tift MS, Riet-Sapriza F et al (2016) Regional variability in diving physiology and behavior in a widely distributed air-breathing marine predator, the South American sea lion (*Otaria byronia*). J Exp Biol 219:2320–2330. doi:10.1242/jeb.138677

Huggenberger S, Rauschmann MA, Oelschläger HHA (2008) Functional morphology of the hyolaryngeal complex of the harbor porpoise (*Phocoena phocoena*): implications for its role in sound production and respiration. Anat Rec 291:1262–1270. doi:10.1002/ar.20745

Huggenberger S, Rauschmann MA, Vogl TJ, Oelschläger HHA (2009) Functional morphology of the nasal complex in the harbor porpoise (*Phocoena phocoena* L.). Anat Rec 292:902–920. doi:10.1002/ar.20854

Kanatous SB, Dimichele LV, Cowan DF, Davis RW (1999) High aerobic capacities in the skeletal muscles of pinnipeds: adaptations to diving hypoxia. J Appl Physiol 86:1247–1256

Kielhorn CE, Dillaman RM, Kinsey ST et al (2013) Locomotor muscle profile of a deep (*Kogia breviceps*) versus shallow (*Tursiops truncatus*) diving cetacean. J Morphol 274:663–675. doi:10.1002/jmor.20124

Kooyman GL (1989) Diverse divers. Springer, New York

Kuhn M, Weston S, Wing J, Forester J (2013) The contrast package

LaFramboise WA, Daood MJ, Guthrie RD et al (1991) Emergence of the mature myosin phenotype in the rat diaphragm muscle. Dev Biol 144:1–15

Lammers MO, Castellote M (2009) The beluga whale produces two pulses to form its sonar signal. Biol Lett 5:297–301. doi:10.1098/rsbl.2008.0782

Lawrence B, Schevill WE (1956) The functional anatomy of the delphinid nose. Bull Mus Comp Zool 114:103–182

Lawrence B, Schevill WE (1965) Gular musculature in delphinids. Bull Mus Comp Zool Harvard Univ 133:1–65

Liste F, Palacio J, Ribes V et al (2006) Anatomic and computed tomographic atlas of the head of the newborn bottlenose dolphin (*Tursiops truncatus*). Vet Radiol Ultrasound 47:453–460. doi:10.1111/j.1740-8261.2006.00167.x

Liu Y, Jia S, Hou Y (2009) Effects of ovariectomy on rat genioglossal muscle contractile properties and fiber-type distribution. Angle Orthod 79:509–514. doi:10.2319/031608-149.1

Madsen PT, Wisniewska DM, Beedholm K (2010) Single source sound production and dynamic beam formation in echolocating harbour porpoises (*Phocoena phocoena*). J Exp Biol 213:3105–3110. doi:10.1242/jeb.044420

Madsen PT, Lammers M, Wisniewska D, Beedholm K (2013) Nasal sound production in echolocating delphinids (*Tursiops truncatus* and *Pseudorca crassidens*) is dynamic, but unilateral: clicking on the right side and whistling on the left side. J Exp Biol 216:4091–4102. doi:10.1242/jeb.091306

Marsh RL, Taigen TL (1987) Properties enhancing aerobic capacity of calling muscles in gray tree frogs Hyla versicolor. Am J Physiol 252:R786–R793

Mead JG (1975) Anatomy of the external nasal passages and facial complex in the Delphinidae (Mammalia: Cetacea). Smithson Contrib to Zool 1–72. doi:10.5479/si.00810282.207

Melcón ML, Cummins AJ, Kerosky SM et al (2012) Blue whales respond to anthropogenic noise. PLoS One 7:1–6. doi:10.1371/journal.pone.0032681

Mu L, Sanders I (2002) Muscle fiber-type distribution pattern in the human cricopharyngeus muscle. Dysphagia 17:87–96. doi:10.1007/s00455-001-0108-2

Noren SR (2004) Buffering capacity of the locomotor muscle in cetaceans: correlates with postpartum development, dive

duration, and swim performance. Mar Mammal Sci 20:808–822. doi:10.1111/j.1748-7692.2004.tb01194.x
Noren SR, Williams TM (2000) Body size and skeletal muscle myoglobin of cetaceans: adaptations for maximizing dive duration. Comp Biochem Physiol A 126:181–191. doi:10.1016/S1095-6433(00)00182-3
Noren SR, Williams TM, Pabst DA et al (2001) The development of diving in marine endotherms: preparing the skeletal muscles of dolphins, penguins, and seals for activity during submergence. J Comp Physiol B 171:127–134. doi:10.1007/s003600000161
Noren SR, Lacave G, Wells RS, Williams TM (2002) The development of blood oxygen stores in bottlenose dolphins (*Tursiops truncatus*): implications for diving capacity. J Zool Lond 258:105–113. doi:10.1017/S0952836902001243
Noren DP, Holt MM, Dunkin RC, Williams TM (2013) The metabolic cost of communicative sound production in bottlenose dolphins (*Tursiops truncatus*). J Exp Biol 216:1624–1629. doi:10.1242/jeb.083212
Noren SR, Noren DP, Gaydos JK (2014) Living in the fast lane: rapid development of the locomotor muscle in immature harbor porpoises (*Phocoena phocoena*). J Comp Physiol B 184:1065–1076. doi:10.1007/s00360-014-0854-8
Ophir AG, Schrader SB, Gillooly JF (2010) Energetic cost of calling: general constraints and species-specific differences. J Evol Biol 23:1564–1569. doi:10.1111/j.1420-9101.2010.02005.x
Pattengale PK, Holloszy JO (1967) Augmentation by a program of skeletal muscle myoglobin of treadmill running. Am J Physiol 213:783–785
Petrof BJ, Kelly AM, Rubinstein NA, Pack AI (1992) Effect of hypothyroidism on myosin heavy chain expression in rat pharyngeal dilator muscles. J Appl Physiol 73:179–187
Piscitelli MA, McLellan WA, Rommel SA et al (2010) Lung size and thoracic morphology in shallow- and deep-diving cetaceans. J Morphol 271:654–673. doi:10.1002/jmor.10823
Ponganis PJ (2011) Diving mammals. Compr Physiol 1:517–535. doi:10.1002/cphy.c091003
Ponganis PJ, Pierce RW (1978) Muscle metabolic profiles and fiber-type composition in some marine mammals. Comp Biochem Physiol 59:7–10
Ponganis PJ, Costello ML, Starke LN et al (1997) Structural and biochemical characteristics of locomotory muscles of emperor penguins, *Aptenodytes forsteri*. Respir Physiol 109:73–80
Reynafarje B (1963) Simplified method for the determination of myoglobin. J Lab Clin Med 61:138–145
Richmond JP, Burns JM, Rea LD (2006) Ontogeny of total body oxygen stores and aerobic dive potential in Steller sea lions (*Eumetopias jubatus*). J Comp Physiol B 176:535–545. doi:10.1007/s00360-006-0076-9
Ridgway SH, Carder DA, Green RF et al (1980) Electromyographic and pressure events in the nasolaryngeal system of dolphins during sound production. In: Busnel R, Fish JF (eds) Anim. Sonar Syst. Plenum Press, New York, pp 239–250
Ridgway SH, Carder DA, Kamolnick T et al (2001) Hearing and whistling in the deep sea: depth influences whistle spectra but does not attenuate hearing by white whales (*Delphinapterus leucas*) (Odontoceti, Cetacea). J Exp Biol 204:3829–3841
Ridgway S, Samuelson Dibble D, Van Alstyne K, Price D (2015) On doing two things at once: dolphin brain and nose coordinate sonar clicks, buzzes and emotional squeals with social sounds during fish capture. J Exp Biol 218:3987–3995. doi:10.1242/jeb.130559
Rome LC (2006) Design and function of superfast muscles: new insights into the physiology of skeletal muscle. Ann Rev Physiol 68:193–221. doi:10.1146/annurev.physiol.68.040104.105418
Rome LC, Syme DA, Hollingworth S et al (1996) The whistle and the rattle: the design of sound producing muscles. Proc Natl Acad Sci USA 93:8095–8100. doi:10.1073/pnas.93.15.8095
Saigusa H, Niimi S, Yamashita K et al (2001) Morphological and histochemical studies of the genioglossus muscle. Ann Otol Rhinol Laryngol 110:779–784
Sassoon DA, Gray GE, Kelley DB (1987) Androgen regulation of muscle fiber type in the sexually dimorphic larynx of *Xenopus laevis*. J Neurosci 7:3198–3206
Schiaffino S, Gorza L, Ausoni S, Bottinelli R, Reggiani C, Larson L, Edstrom L, Gundersen K, Lomo T (1990) Muscle fiber types expressing different myosin heavy chain isoforms. Their functional properties and adaptive capacity. In: Schiaffino S, Gorza L, Ausoni S (eds) The dynamic state of muscle fibers: proceedings of the international symposium. Walter de Gruyter, Berlin, pp 329–341
Schrøder HD, Reske-Nielsen E (1983) Fiber types in the striated urethral and anal sphincters. Acta Neuropathol 60:278–282
Shero MR, Andrews RD, Lestyk KC, Burns JM (2012) Development of the aerobic dive limit and muscular efficiency in northern fur seals (*Callorhinus ursinus*). J Comp Physiol B 182:425–436. doi:10.1007/s00360-011-0619-6
Smith KK (1989) Histological demonstration of muscle spindles in the tongue of the rat. Arch Oral Biol 34:529–534. doi:10.1016/0003-9969(89)90091-5
Sutlive TG, McClung JR, Goldberg SJ (1999) Whole-muscle and motor-unit contractile properties of the styloglossus muscle in rat. J Neurophysiol 82:584–592
Sutlive TG, Shall MS, McClung JR, Goldberg SJ (2000) Contractile properties of the tongue's genioglossus muscle and motor units in the rat. Muscle Nerve 23:416–425
Turner DL, Butler PJ (1988) The aerobic capacity of locomotory muscles in the tufted duck, Aythya fuligula. J Exp Biol 135:445–460
Tyack PL, Miller EH (2002) Vocal anatomy, acoustic communication and echolocation. In: Hoelzel AR (ed) Mar. Mammal Biol. an Evol. Approach, 1st edn. Blackwell Science Ltd, Malden, pp 142–184
Velten BP, Dillaman RM, Kinsey ST et al (2013) Novel locomotor muscle design in extreme deep-diving whales. J Exp Biol 216:1862–1871. doi:10.1242/jeb.081323
Villegas-Amtmann S, Costa DP (2010) Oxygen stores plasticity linked to foraging behaviour and pregnancy in a diving predator, the Galapagos sea lion. Funct Ecol 24:785–795. doi:10.1111/j.1365-2435.2009.01685.x
Villegas-Amtmann S, Atkinson S, Paras-Garcia A, Costa DP (2012) Seasonal variation in blood and muscle oxygen stores attributed to diving behavior, environmental temperature and pregnancy in a marine predator, the California sea lion. Comp Biochem Physiol A 162:413–420. doi:10.1016/j.cbpa.2012.04.019
Weilgart LS (2007) The impacts of anthropogenic ocean noise on cetaceans and implications for management. Can J Zool 85:1091–1116. doi:10.1139/Z07-101
Weise MJ, Costa DP (2007) Total body oxygen stores and physiological diving capacity of California sea lions as a function of sex and age. J Exp Biol 210:278–289. doi:10.1242/jeb.02643
Werth AJ (2007) Adaptations of the cetacean hyolingual apparatus for aquatic feeding and thermoregulation. Anat Rec 290:546–568. doi:10.1002/ar.20538
Williams TM (1999) The evolution of cost efficient swimming in marine mammals: limits to energetic optimization. Philos Trans R Soc Lond B 354:193–201
Williams TM, Friedl WA, Haun JE (1993) The physiology of bottlenose dolphins (*Tursiops truncatus*): heart rate, metabolic rate and plasma lactate concentration during exercise. J Exp Biol 179:31–46

Williams CT, Sheriff MJ, Schmutz JA et al (2011a) Data logging of body temperatures provides precise information on phenology of reproductive events in a free-living arctic hibernator. J Comp Physiol B 181:1101–1109. doi:10.1007/s00360-011-0593-z

Williams TM, Noren SR, Glenn M (2011b) Extreme physiological adaptations as predictors of climate-change sensitivity in the narwhal, *Monodon monoceros*. Mar Mammal Sci 27:334–349. doi:10.1111/j.1748-7692.2010.00408.x

Yeates LC, Williams TM, Fink TL (2007) Diving and foraging energetics of the smallest marine mammal, the sea otter (*Enhydra lutris*). J Exp Biol 210:1960–1970. doi:10.1242/jeb.02767